PCCP

ROYAL SOCIETY OF CHEMISTRY

PAPER

View Article Online
View Journal | View Issue

Cite this: *Phys. Chem. Chem. Phys.*, 2025, **27**, 7199

Chemical and biological incorporation of the blue florescent amino acid 4-cyanotryptophan into proteins: application to tune the absorption and emission wavelengths of GFP†

Manxi Wang and Feng Gai *

Received 10th January 2025,
Accepted 13th March 2025

DOI: 10.1039/d5cp00112a

rsc.li/pccp

4-Cyanotryptophan is a blue fluorescent unnatural amino acid (UAA) that not only has a large fluorescence quantum yield (>0.8) and a long fluorescence lifetime (>13 ns) in water but is also chemically and photophysically stable, making it a valuable UAA-based fluorophore in biological spectroscopy and microscopy. However, its broad utility requires further development of simple methods for introducing this UAA into large proteins. Herein, we demonstrated two such methods, one is based on a post-translational modification strategy and the other is based on a selective pressure incorporation approach. In addition, in a proof-of-principle application, we demonstrated that incorporation of this UAA at the 66 position of a green fluorescent protein (GFP) variant can modify its photophysical properties.

1. Introduction

Recently, Hilaire *et al.*[1] demonstrated that 4-cyanotryptophan (4CN-Trp), a simple derivative of the naturally-occurring aromatic amino acid, tryptophan (Trp), exhibits unique photophysical properties: its absorption spectrum is redshifted from that of Trp and extends beyond 360 nm, its emission spectrum locates in the blue region of the visible light spectrum, it has a large fluorescence quantum yield (>0.8 in water), its fluorescence decay follows first-order kinetics with a relatively long lifetime (*ca.* 13 ns in water), and it is photostable. Therefore, 4CN-Trp can serve as an amino acid-based fluorescence probe in biological spectroscopy and microscopy.[2] For example, it has been used to (1) image peptide-membrane interactions,[3,4] (2) assess protein conformational dynamics[5–7] and protein local electric field,[8,9] (3) visualize the cellular localization of cell penetrating peptides *via* confocal microscopy,[10] (4) assess the hydration status of the Trp41 gate of the influenza M2 proton channel,[11] (5) image platelet integrins *via* two-photon microscopy,[12] and (6) assess how vacuolar pH controls vacuolar metabolite levels.[13] However, to make this blue fluorescent unnatural amino acid (UAA) more broadly useful, methods that can incorporate it into proteins are needed.[14] Herein, we demonstrated two such methods.

As shown (Scheme 1), the first method is chemically based, which utilizes an alkylation reaction to append a 4-cyanoindole (4CNI) moiety, which is the chromophore of 4CN-Trp, to the desired protein *via* a free sulfhydryl group (–SH) of a cysteine (C) residue. Because the underlying SN2 reaction is relatively simple and can be carried out under mild conditions with good yield, it has been used to incorporate various small-sized spectroscopic probes, such as boron dipyrromethene difluoride (BODIPY) fluorescent probes,[15,16] nitrile-based NMR probes,[17] and an ester infrared probe[18] into proteins.

As shown (Scheme 2), the second method is biologically based, which employs the selective pressure incorporation (SPI) method to incorporate 4CN-Trp (the L-form) into the protein of interest. The SPI method[19] relies on the promiscuity of a natural aminoacyl-tRNA synthetase (AARS) to recognizes a UAA for protein translation. This method is most effective when an auxotroph is used, because it requires a specific amino acid to be supplied exogenously and therefore an analogue of this amino acid can be used for substitution. Because its simplicity in practice, the SPI method has been widely used to incorporate various UAAs into proteins in a residue-specific manner. In particular, tryptophan-autotrophs have been used to introduce

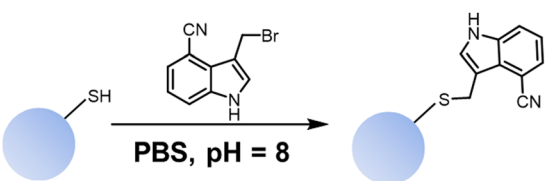

Scheme 1 The alkylation reaction used to append the fluorophore of 4CN-Trp to the protein (blue sphere) of interest.

Beijing National Laboratory for Molecular Sciences, College of Chemistry and Molecular Engineering, Peking University, Beijing 100871, China.
E-mail: fgai@pku.edu.cn

† Electronic supplementary information (ESI) available. See DOI: https://doi.org/10.1039/d5cp00112a

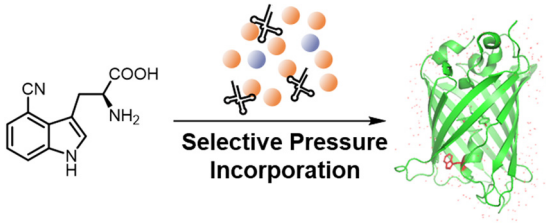

Scheme 2 The biologically based method used to incorporate 4CN-Trp to proteins.

various Trp analogues into different proteins. For example, Bronskill and Wong incorporated fluorine-substituted Trps into ribosomal proteins to suppress the intrinsic fluorescence of Trp and to facilitate the spectroscopic investigation of other chromophores,[20] Boknevitz *et al.*[21] incorporated a boron and nitrogen-containing tryptophan analogue into superfolder GFP (sfGFP) to serve as a fluorescent probe, and Ohler *et al.*[22] incorporated 4-fluoro-5-hydroxytryptophan and 6-fluoro-5-hydroxytryptophan into Azurin to serve as EPR probes.

In the current study, we used sfGFP as our model system to first test whether 4CN-Trp can be incorporate into proteins *via* the SPI method. This is because sfGFP can be highly expressed in *E. coli*[23] and contains only one Trp residue (*i.e.*, Trp57). Subsequently, we employed cerulearn (pdb ID: 2WSO),[24] which is a variant of enhanced cyan fluorescent protein (eCFP)[25] that consists of a Trp-based chromophore, to show that 4CN-Trp can potentially be used to develop fluorescent proteins with different photophysical characteristics. Our results demonstrated that 4CN-Trp not only can be incorporated into both protein systems, but it can also be used to tune their absorption and emission properties.

2. Experimental details

2.1. Materials

All chemicals were commercially purchased and used as received. Specifically, 4-cyano-L-tryptophan (97%) was purchased from Amatek Scientific Co. Ltd (Suzhou, China). 4-Cyanoindole (98%), tosyl chloride, and all anhydrous solvents were purchased from J&K Scientific Co., Ltd (Beijing, China). Phosphorus tribromide and $POCl_3$ were purchased from Anhui Zesheng Technology Co., Ltd. All organic solvents used are chromatographic grade or higher. Deuterated solvents were purchased from Energy Chemical (Shanghai) Co., Ltd Deionized water ($\geq$18 MΩ cm) was obtained from a Milli-Q Direct water purification system.

The peptide used in the current study was synthesized *via* standard 9-fluorenylmethoxy-carbonyl (Fmoc) solid phase peptide synthesis method and purified by reverse-phase high-performance liquid chromatography on an Agilent Technologies 1260 Infinity equipped with a C18 column. The masses of the unlabelled and labelled peptides were verified using a liquid chromatography mass spectrometer from Waters. All proteins were purified by AKTA fast protein liquid chromatography equipped with desalting column and His Trap HP column. For spectroscopic measurements, protein samples were prepared in PBS buffer (50 mM, pH = 7.4).

2.2. Absorption measurements

UV-Vis absorption spectra were collected on a Cary 60 UV-Vis spectrophotometer (Agilent) at room temperature using a quartz cuvette of 1.0 cm optical path length, and the sample concentrations were in the range of 50–100 μM.

2.3. Fluorescence measurements and quantum yield (QY) determination

Steady-state fluorescence measurements were carried out on an FLS980 fluorometer (Edinburgh Instruments) at room temperature using a quartz cuvette of 1.0 cm optical path length and the following instrument parameters: 2.5 nm/2.5 nm excitation/emission slits for peptide solutions, 2.5 nm/5.0 nm excitation/emission slits for protein solutions, 1.0 nm s^{-1} integration time, and an excitation wavelength (λ_{ex}) of 325 nm, 340 nm, or 420 nm.

Time-resolved fluorescence measurements were carried out on a FLS980 time-correlated single-photon counting (TCSPC) apparatus (Edinburgh Instruments). Fluorescence excitation at 405 nm was achieved by an EPL-405 laser, and fluorescence emission was collected at 480 nm. The time base was set to be 0–60 ns with a total of 2048 channels and the maximum peak count was set at 10 000. The fluorescence decay kinetics were analyzed by the F980 software using an instrument response function (IRF) determined by measuring the scattering light from a silica solution under the same experimental conditions. In addition, the optical density (OD) of the sample at the excitation wavelength of 405 nm was in the range of 0.10–0.15.

The fluorescence QY of a particular sample was determined using the following equation:

$$QY_s = QY_r \frac{S_s}{S_r}\left(\frac{n_s}{n_r}\right)^2$$

where n represents the refractive index of the solvent, S represents the slope of the I_F *versus* I_{abs} plot, where I_F represents the integrated fluorescence intensity of the fluorescence spectrum and I_{abs} is a quantity that is proportional to the absorbed light intensity at the fluorescence excitation wavelength (λ_{ex} = 325 nm or 420 nm),[26] and the subscript represents the sample (s) and reference (r), respectively. In the current study, 9,10-diphenylanthracene (DPA, QY = 0.90 in cyclohexane at λ_{ex} = 325 nm) and fluorescein (QY = 0.79 in ethanol at λ_{ex} = 420 nm) were used as the references.

2.4. Other measurements, chemical synthesis, and protein expression protocols

The details of all other experimental measurements, chemical synthesis, and protein expression are given in the ESI.†

3. Results and discussion

3.1. Chemical incorporation of 4CN-Trp into proteins

As shown (Scheme 3), in the current case the chromophore-containing reactant of the alkylation reaction, 3-(bromomethyl)-1*H*-indole-4-carbonitrile (3B4CNI), was prepared from 4CNI in five steps (see the ESI,† for details). Specifically, 3-formyl-1*H*-indole-4-carbonitrile (**2**) was first synthesized from 4CNI (**1**) *via*

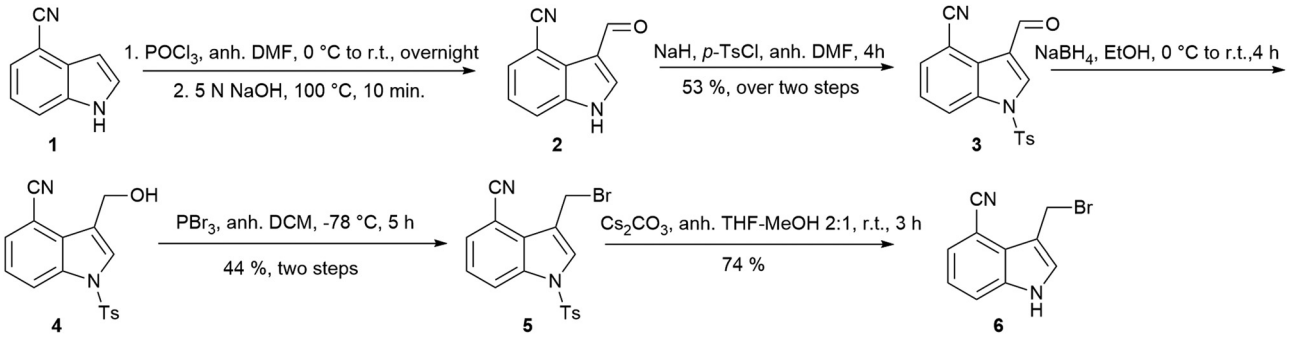

Scheme 3 Synthesis route of 3B4CNI.

the Vilsmeier-Haack reaction, the N–H group of which was then protected by Tosyl chloride and the aldehyde group of the corresponding product (**3**) was reduced to produce 3-(hydroxymethyl)-1-tosyl-1*H*-indole-4-carbonitrile (**4**). Subsequently, the hydroxyl group of **4** was brominated to form 3-(bromomethyl)-1-tosyl-1*H*-indole-4-carbonitrile (**5**), which was further deprotected to yield 3B4CNI (**6**).

To demonstrate the feasibility of using 3B4CNI to carry out the aforementioned cysteine alkylation reaction, we first tested its reaction efficiency with a short peptide that contains a single cysteine residue (sequence: YGGCGG). We found that, as expected, 3B4CNI can react with YGGCGG quickly under mild conditions (*i.e.*, in PBS buffer of pH 8.0 and at 37 °C, see the ESI,† for details). For example, through the use of mass spectrometry as a means to monitor the progress of the reaction, we found that, at a 3B4CNI/peptide molar ratio of 10 : 1, the yield of the alkylation reaction can reach up to *ca.* 95% in three hours (Fig. S1 in the ESI†). In addition, we found that in the presence of 8 M urea, which is commonly used to unfold proteins, this reaction also works well (Fig. S2 in the ESI†), suggesting that 3B4CNI can also be used to react with cysteine residues that are buried in the interior of the protein of interest under denaturation conditions.

As shown (Fig. 1A and Fig. S3 in the ESI†), the absorption spectrum of the 4CNI-labelled YGGCGG peptide (hereafter referred to as YGGC*GG) is similar to that of $GW_{CN}G$ (where W_{CN} represents 4CN-Trp). However, the maximum emission wavelength (λ_{em}) of the 4CNI fluorophore in YGGC*GG is at *ca.* 437 nm, which is redshifted by *ca.* 15 nm from that of the 4CNI fluorophore in $GW_{CN}G$ (Fig. 1B and Fig. S3 in the ESI†). In addition, the absorption spectrum of YGGC*GG is insensitive to solvent (Fig. S4 in the ESI†), and its fluorescence QYs measured in different solvents, including H_2O, ethanol (EtOH), isopropanol (IPA) and tetrahydrofuran (THF), are similar (Fig. S5 and Table S1 in the ESI†). For example, the QY values were determined to be 0.21 ± 0.03 in H_2O and 0.23 ± 0.07 in THF, respectively. Taken together, these results indicate that the sulfur atom on the sidechain can significantly affect the photophysical property of 4CNI. Nevertheless, as observed for 4CNI and 4CN-Trp,[9] the λ_{em} value of YGGC*GG exhibits a sensitive dependence on solvent (Fig. 1B), suggesting that the 4CNI fluorophore thus appended on a protein could also be used as a fluorescence probe of local electric field.[9]

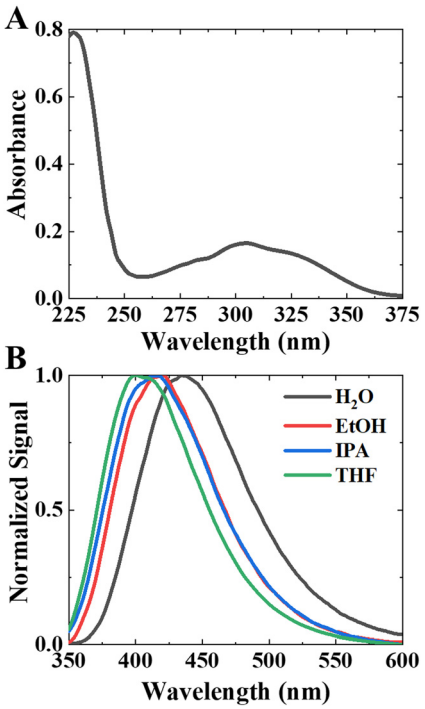

Fig. 1 (A) Absorption spectrum of YGGC*GG in H_2O. (B) Normalized fluorescence spectra of YGGC*GG in H_2O, EtOH, IPA and THF, as indicated. These data were obtained with an λ_{ex} of 325 nm.

Next, we tested the utility of 3B4CNI to incorporate a 4CNI fluorophore into large protein systems (see the ESI,† for details). Specifically, we chose bovine serum albumin (BSA) as it is easily available and has only one free cysteine residue (*i.e.*, Cys34). Moreover, Cys34 is only partially exposed to solvent, making the test more representative. Specifically, the BSA solution was prepared in phosphate buffer (pH 8.0, 50 mM) with a concentration of 13.2 mg mL^{-1} and the alkylation reaction was started by mixing a 100 μL of this BSA solution with a 3B4CNI solution (4.6 mg in 10 μL DMF). Then, the resultant reaction mixture was vortexed and shaken vigorously for 3 hours at 37 °C. Subsequently, the solid in the reaction mixture was removed by centrifugation (5 min, 4 °C, 10 000 rpm), followed by removal of the unreacted 3B4CNI in the supernatant by an AKTA FPLC desalting column. Then, the protein-containing solution, which

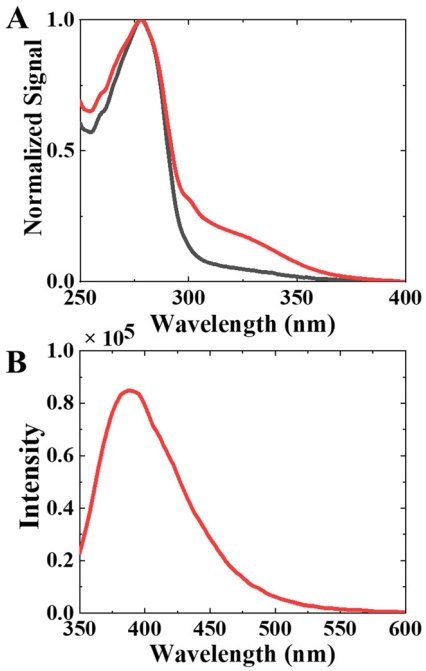

Fig. 2 (A) Normalized absorption spectra of BSA (black) and 4CNI-labelled BSA (red) in H_2O. (B) Fluorescence spectrum of 4CNI-labelled BSA in H_2O, obtained with an λ_{ex} of 325 nm.

contains the labelled BSA and unlabelled BSA molecules, was lyophilized and the resultant powders were used in the subsequent experiments.

The relevant mass spectrometry results exhibit a mass difference of *ca.* 160 Da, indicating the successful labelling (Fig. S6 in the ESI†). As shown (Fig. 2A), the absorption spectrum of the labelled BSA further confirms the successful incorporation of the 4CNI chromophore into the protein, since in the wavelength range of >300 nm it exhibits the characteristics of the absorption spectrum of YGGC*GG. Similarly, the fluorescence spectrum of the labelled BSA in H_2O, obtained with an λ_{ex} of 325 nm, also corroborates this notion (Fig. 2B). This is because the other native aromatic amino acids in BSA have a negligible absorbance at 325 nm; hence the fluorescence must arise from the 4CNI fluorophore. Moreover, the λ_{em} (415 nm) of the 4CNI-labelled BSA is blue-shifted *ca.* 22 nm from that (437 nm) of 4CNI-labelled peptide in H_2O (Fig. 1B), which is consistent with the fact that the Cys34 is partially buried in BSA.

3.2. Biological incorporation of 4CN-Trp into GFP

In the current study, we chose superfolder GFP (sfGFP, pdb ID: 2B3P) as our model protein because it contains a single tryptophan residue at position 57 as well as a tryptophan-auxotrophic *E. coli* strain,[27] which was purchased from ATCC (catalog number: 49980), for protein expression. Specifically, all fermentation and expression experiments were performed in GMML medium supplemented with 200 μM glucose,[21] and the host *E. coli* was routinely transformed with plasmid pET22b-sfGFP (with a His-tag at the N-terminus of the protein) using standard cloning methods (see the ESI,† for the details of protein expression).

Result from SDS-PAGE analysis, which shows the existence of a ~27 kDa protein (Fig. S7 in the ESI†), indicates that sfGFP can be successfully expressed in media that contains 4CN-Trp but no Trp and that 4CN-Trp is recognized by the AARSs from the auxotrophic strain and the native Trp residue is mutated to 4CN-Trp. As shown (Table S2 in the ESI†), mass spectroscopic measurements on the expressed protein (hereafter refeed to as 4CN-Trp-sfGFP) also confirm that it contains a 4CN-Trp residue. Further spectroscopic measurements on 4CN-Trp-sfGFP provide additional supporting evidences. As indicated (Fig. 3A), compared to that of sfGFP, the absorption spectrum of 4CN-Trp-sfGFP contains an additional band in the 300–350 nm region, which is characteristic of the absorption feature of 4CN-Trp. Interestingly, the fluorescence spectrum of 4CN-Trp-sfGFP obtained with an λ_{ex} of 340 nm, where the intrinsic fluorophore of sfGFP has a minimum absorbance, indicates that the 4CN-Trp is only weakly emissive in this case (Fig. 3B). However, in comparison to that of the fluorescence spectrum of sfGFP of equal concentration, the intensity of the intrinsic sfGFP fluorescence spectrum of 4CN-Trp-sfGFP is significantly increased (Fig. 3B). This indicates that the 4CN-Trp fluorescence is significantly quenched by the intrinsic fluorophore of sfGFP, likely through a fluorescence resonance energy transfer (FRET) mechanism. This is consistent with the fact that the fluorescence spectrum of 4CN-Trp completely overlaps with the absorption spectrum arising from the intrinsic chromophore of sfGFP as well as with the fact that, according to the crystal structure of sfGFP,[23] the Trp57 residue is only *ca.* 13.0 Å away

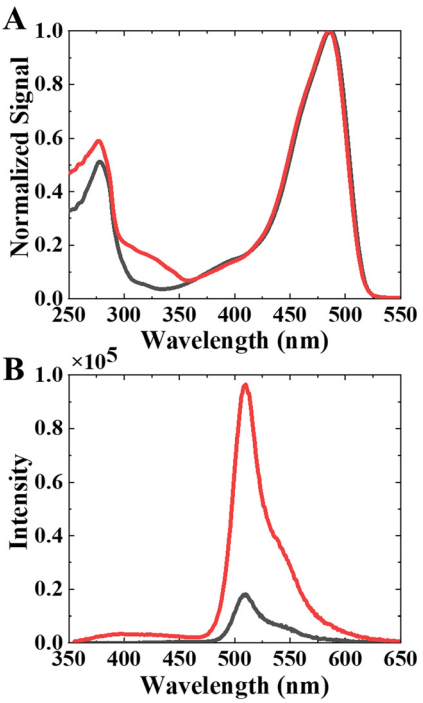

Fig. 3 (A) Normalized absorption spectra of sfGFP (black) and 4CN-Trp-sfGFP (red) in PBS buffer (pH = 7.4). (B) Concentration-normalized fluorescence spectra of sfGFP (black) and 4CN-Trp-sfGFP (red) in PBS buffer (pH = 7.4), measured with an λ_{ex} of 340 nm.

from this chromophore. Finally, the fluorescence spectrum of the 4CN-Trp residue in 4CN-Trp-sfGFP is peaked at 397 nm, indicating that it is situated in a dehydrated environment, which is consistent with the fact that Trp57 is buried. Taken together, our results not only confirm that 4CN-Trp can be incorporated into proteins *via* the SPI method but also indicate that in the case of sfGFP (or similar GFP variants) the Trp to 4CN-Trp mutation can effectively increase the overall brightness of the chromophore in the 300–350 nm excitation wavelength region.

3.3. Application to tune the photophysical property of Cerulean

Ever since the discovery of GFP, tremendous efforts have been made to tune its photophysical property, such as its absorption and emission spectra, aiming to broaden its utility in biological spectroscopy and microscopy.[28–30] One particularly useful strategy is to modify the chromophore by mutating the amino acids that are involved in the formation of the native chromophore in GFP. For example, Tsien and co-workers[31] demonstrated that when Y66 was mutated to His or Trp, the absorption spectrum of the resultant proteins (*e.g.*, Y66W) is blue-shifted from that of GFP, making it useful as a FRET donor to GFP.[32] Further mutations at other sites led to the development of various blue fluorescent proteins, such as the enhanced blue fluorescent protein (ECFP)[25,33] and Cerulearn.[24] In comparison to ECFP, it was noted that Cerulearn has an enhanced fluorescence QY and brightness. Besides canonical amino acids, a wide variety of unnatural amino acids (UAAs) have also been employed to generate GFP variants that exhibit different biophysical characteristics.[34–37]

Because nitrile is a strong electron-withdrawing group,[38] we hypothesize that replacing the Trp66 residue with 4CN-Trp in Cerulean can further tune its absorption and emission properties. As shown (Table S3 in the ESI†), the two native Trp residues in Cerulean can be successfully replaced by 4CN-Trp using *E. coli* ATCC49980 that was routinely transformed with plasmid: pET22b-Cerulean (with a His-tag at the protein C-terminus) and the same expression protocols described above for sfGFP, except that that in the current case a lower induction temperature (27 °C) and a longer incubation time (24 h) were used.

As indicated (Fig. 4), the 4CN-Trp-containing Cerulean (hereafter referred to as 4CN-Trp-Cerulean) indeed exhibits different photophysical behaviors from Cerulean. Specifically, (1) its absorption spectrum is blue-shifted by *ca.* 25 nm from that of Cerulen, with an λ_{ab} of *ca.* 413 nm; (2) its fluorescence spectrum becomes narrower and is also blue-shifted (*ca.* 8 nm) from that of cerulean; (3) its fluorescence QY (0.32 ± 0.08; determined with an λ_{ex} of 420 nm; Fig. S8 in the ESI†) is lower than that of Cerulean (0.49);[39] and (4) while similar to that observed for Cerulean, a double-exponential function is required to describe the fluorescence decay kinetics of 4CN-Trp-Cerulean (Fig. S9 in the ESI†), the decay lifetimes (τ_1 = 0.8 ± 0.1 ns and τ_2 = 3.1 ± 0.1 ns) are different from those of Cerulean (τ_1 = 2.3 ns and τ_2 = 4.5 ns).[25] Therefore, taken together, these results confirm our hypothesis that 4CN-Trp can be used to more effectively modify the photophysical properties of fluorescent proteins, compared to Trp.

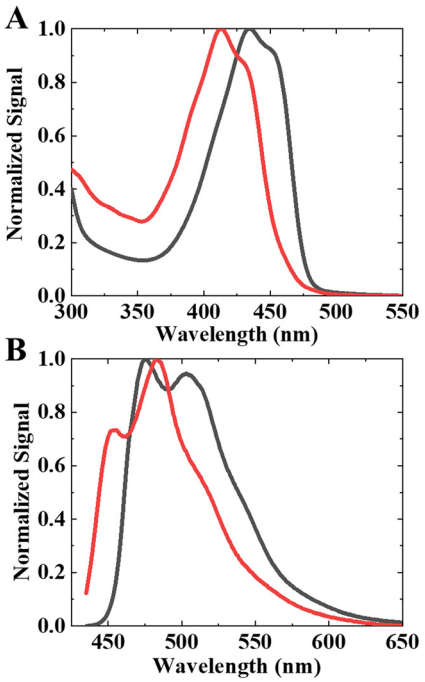

Fig. 4 (A) Normalized absorption spectra of Cerulean (black) and 4CN-Trp-Cerulean (red) in PBS buffer (pH = 7.4). (B) Normalized fluorescence spectra of Cerulean (black) and 4CN-Trp-Cerulean (red) in PBS buffer (pH = 7.4), measured with an λ_{ex} of 420 nm.

4. Conclusions

In summary, we demonstrated two simple methods to incorporate a 4CNI-based blue fluorophore into proteins. The first one employed cysteine alkylation, which is commonly used to label proteins in proteomics[40] and in biophysics,[41] to introduce a 4CNI moiety in a site-specific manner, whereas the second one took advantage of a Trp auxotrophic expression strain of *E. coli* to directly mutate the Trp residue(s) in the protein of interest to 4CN-Trp. While this selective pressure incorporation method lacks site specificity when multiple Trp residues are present, we believe that it is still widely useful. This is because Trp is one the least abundant amino acids in proteins and, as a result, many proteins do not contain Trp.[42,43] Therefore, a 4CN-Trp can be site-specifically incorporated into proteins that lack of Trp through this biological method in conjunction with site-specific protein mutagenesis (*i.e.*, mutating the native amino acid at the desired site to Trp at the genetic level). Given the proven spectroscopic and imaging utilities of 4CN-Trp, we believe that the two incorporation methods we developed in this study will find broad utility in biological spectroscopy and microscopy. In addition, as an example, we demonstrated that 4CN-Trp can be used to tune the photophysical properties of GFP.

Data availability

The data supporting this article have been included as part of the ESI.†

Conflicts of interest

There are no conflicts to declare.

Acknowledgements

We acknowledge support from the National Natural Science Foundation of China (22333001 and 22350710183).

References

1 M. R. Hilaire, I. A. Ahmed, C.-W. Lin, H. Jo, W. F. DeGrado and F. Gai, *Proc. Natl. Acad. Sci. U. S. A.*, 2017, **114**, 6005–6009.
2 R.-r Feng, M. Wang, W. Zhang and F. Gai, *Chem. Rev.*, 2024, **124**, 6501–6542.
3 K. Zhang, I. A. Ahmed, H. T. Kratochvil, W. F. DeGrado, F. Gai and H. Jo, *Chem. Commun.*, 2019, **55**, 5095–5098.
4 Y. Wu, M. T. Bertran, J. Rowley, E. D. D. Calder, D. Joshi and L. J. Walport, *ChemMedChem*, 2021, **16**, 3185–3188.
5 L. J. G. W. van Wilderen, H. Brunst, H. Gustmann, J. Wachtveitl, J. Broos and J. Bredenbeck, *Phys. Chem. Chem. Phys.*, 2018, **20**, 19906–19915.
6 I. A. Ahmed, J. M. Rodgers, C. Eng, T. Troxler and F. Gai, *Phys. Chem. Chem. Phys.*, 2019, **21**, 12843–12849.
7 M. Wang, B. Zhuang, K. Tang, R.-R. Feng and F. Gai, *J. Phys. Chem. Lett.*, 2024, **15**, 11723–11729.
8 T. Haldar, S. Chatterjee, M. N. Alam, P. Maity and S. Bagchi, *J. Phys. Chem. B*, 2022, **126**, 10732–10740.
9 Y. Yang, R.-r Feng and F. Gai, *J. Phys. Chem. B*, 2023, **127**, 514–519.
10 A. Acharyya, I. A. Ahmed and F. Gai, in *Methods in Enzymology*, ed. D. M. Chenoweth, Academic Press, 2020, vol. 639, pp. 191–215.
11 R. Micikas, A. Acharyya, F. Gai and A. B. Smith, III, *Org. Lett.*, 2021, **23**, 1247–1250.
12 K. P. Fong, I. A. Ahmed, M. Mravic, H. Jo, O. V. Kim, R. I. Litvinov, J. W. Weisel, W. F. DeGrado, F. Gai and J. S. Bennett, *Biochemistry*, 2021, **60**, 1722–1730.
13 V. Okreglak, R. Ling, M. Ingaramo, N. H. Thayer, A. Millett-Sikking and D. E. Gottschling, *Nat. Metab.*, 2023, **5**, 1803–1819.
14 H. Qianzhu, E. H. Abdelkader, A. P. Welegedara, E. Habel, N. Paul, R. L. Frkic, C. J. Jackson, T. Huber and G. Otting, *Angew. Chem., Int. Ed.*, 2025, e202421000.
15 G. A. Baker, S. Pandey, M. A. Kane, T. D. Maloney, A. M. Hartnett and F. V. Bright, *Biopolymers*, 2001, **59**, 502–511.
16 M. S. T. Gonçalves, *Chem. Rev.*, 2009, **109**, 190–212.
17 D. Nonaka, H. Wariishi, K. G. Welinder and H. Fujii, *Biochemistry*, 2010, **49**, 49–57.
18 I. A. Ahmed and F. Gai, *Protein Sci.*, 2017, **26**, 375–381.
19 J. A. Johnson, Y. Y. Lu, J. A. Van Deventer and D. A. Tirrell, *Curr. Opin. Chem. Biol.*, 2010, **14**, 774–780.
20 P. M. Bronskill and J. T. Wong, *Biochem. J.*, 1988, **249**, 305–308.
21 K. Boknevitz, J. S. Italia, B. Li, A. Chatterjee and S.-Y. Liu, *Chem. Sci.*, 2019, **10**, 4994–4998.
22 A. Ohler, H. Long, K. Ohgo, K. Tyson, D. Murray, A. Davis, C. Whittington, E. G. Hvastkovs, L. Duffy, A. Haddy, A. L. Sargent, W. E. Allen and A. R. Offenbacher, *Chem. Commun.*, 2021, **57**, 3107–3110.
23 J.-D. Pédelacq, S. Cabantous, T. Tran, T. C. Terwilliger and G. S. Waldo, *Nat. Biotechnol.*, 2006, **24**, 79–88.
24 M. Lelimousin, M. Noirclerc-Savoye, C. Lazareno-Saez, B. Paetzold, S. Le Vot, R. Chazal, P. Macheboeuf, M. J. Field, D. Bourgeois and A. Royant, *Biochemistry*, 2009, **48**, 10038–10046.
25 M. A. Rizzo, G. H. Springer, B. Granada and D. W. Piston, *Nat. Biotechnol.*, 2004, **22**, 445–449.
26 K. Rurack and M. Spieles, *Anal. Chem.*, 2011, **83**, 1232–1242.
27 E. M. Witkin, *Proc. Natl. Acad. Sci. U. S. A.*, 1963, **50**, 425–430.
28 R. Y. Tsien, *Annu. Rev. Biochem.*, 1998, **67**, 509–544.
29 M. Zimmer, *Chem. Rev.*, 2002, **102**, 759–782.
30 M. G. Romei and S. G. Boxer, *Annu. Rev. Biophys.*, 2019, **48**, 19–44.
31 R. Heim, D. C. Prasher and R. Y. Tsien, *Proc. Natl. Acad. Sci. U. S. A.*, 1994, **91**, 12501–12504.
32 G. H. Patterson, D. W. Piston and B. G. Barisas, *Anal. Biochem.*, 2000, **284**, 438–440.
33 R. Heim and R. Y. Tsien, *Curr. Biol.*, 1996, **6**, 178–182.
34 L. Wang, J. Xie, A. A. Deniz and P. G. Schultz, *J. Org. Chem.*, 2003, **68**, 174–176.
35 S. Chen, Z.-j Chen, W. Ren and H.-w Ai, *J. Am. Chem. Soc.*, 2012, **134**, 9589–9592.
36 J. L. Morris, S. C. Reddington, D. M. Murphy, D. D. Jones, J. A. Platts and E. M. Tippmann, *Org. Lett.*, 2013, **15**, 728–731.
37 C. Fu, T. Kobayashi, N. Wang, C. Hoppmann, B. Yang, R. Irannejad and L. Wang, *J. Am. Chem. Soc.*, 2018, **140**, 11058–11066.
38 R. J. Micikas, I. A. Ahmed, A. Acharyya, A. B. Smith and F. Gai, *Phys. Chem. Chem. Phys.*, 2021, **23**, 6433–6437.
39 G. Gotthard, D. von Stetten, D. Clavel, M. Noirclerc-Savoye and A. Royant, *Biochemistry*, 2017, **56**, 6418–6422.
40 S. Sechi and B. T. Chait, *Anal. Chem.*, 1998, **70**, 5150–5158.
41 M. A. Voinov, D. B. Good, M. E. Ward, S. Milikisiyants, A. Marek, M. A. Caporini, M. Rosay, R. A. Munro, M. Ljumovic, L. S. Brown, V. Ladizhansky and A. I. Smirnov, *J. Phys. Chem. B*, 2015, **119**, 10180–10190.
42 T. Krick, N. Verstraete, L. G. Alonso, D. A. Shub, D. U. Ferreiro, M. Shub and I. E. Sánchez, *Mol. Biol. Evol.*, 2014, **31**, 2905–2912.
43 S. Barik, *Int. J. Mol. Sci.*, 2020, **21**, 8776.

